Laminar Stagnation-Point Heat Transfer for a Two-Temperature Argon Plasma

T.K. Bose* and R.V. Seeniraj†
Indian Institute of Technology, Madras, India

A theory for the heat transfer to the stagnation-point boundary layer of an axisymmetric blunt body in a subsonic two-temperature argon plasma flow was developed. Two-temperature transport properties were calculated from the rigorous kinetic theory and are employed in solving the multifluid problem formulated with a wall sheath boundary condition. The system of equations is solved numerically for various problem parameters. The effects of parameters on thermal nonequilibrium characteristics of the boundary layer are discussed. Also shown are the variations in the transport properties across the boundary layer.

Nomenclature

b = mobility coefficient
C = viscosity-density product ratio, $\rho\mu/(\rho\mu)_0$
$\langle c_p \rangle$ = specific heat of mixture
D = diffusion coefficient
$\boldsymbol{E}$ = electric field
$\boldsymbol{F}$ = ion flux
e = electronic charge
f = dimensionless normal velocity
h = specific mixture enthalpy
H_j = enthalpy of specie, j
i = ionization index, for neutrals $i = 1$
$\boldsymbol{J}$ = current density
k_B = Boltzmann constant
k_{ce}, k_{ch} = pure heat conduction coefficient for electrons and heavies, respectively
k_{re}, k_{rh} = reactive heat conduction coefficient for electrons and heavies, respectively
k_e, k_h = total heat conduction coefficient for electrons and heavies, respectively
k_1-k_6 = constants in Eq. (16)
M = mass of a particle
m = molar mass
N_A = Avogadro number
n = total number density
n_j = number density of j species
p = pressure
Pr = Prandtl number
q = heat flux
R = universal gas constant
Re = Reynolds number
R_w = nose radius of blunt body
r_w = wall radius from the axis of symmetry
s = transformation coordinate in x direction, Eq. (14)
St = Stanton number
T = temperature
U_0 = freestream velocity
u, v = velocity components in x and y directions, respectively
V_j' = diffusion velocity of j species
x_j = mole fraction of j species
x, y = coordinates (Fig. 1)
α = degree of ionization
η = dimensionless coordinate in y direction
μ = viscosity
Γ = volumetric collision frequency
θ = temperature ratio T_e/T_h
ρ = density
φ = plasma sheath potential
σ = electrical conductivity
$\delta_{1,2}$ = defined in Eqs. (23) and (24)
$\delta\varphi$ = potential drop in boundary layer, Eq. (25)
Δ = $T_w/(T_0 - T_w)$
∇ = $\partial/\partial x + \partial/\partial y$

Subscripts

amb = ambipolar
a, n = neutral atom
b = edge of plasma sheath
e = electron
f = field
H = ions plus neutrals
h = heavy particle
i = ion
r = reactive part of heat conductivity coefficient
w = wall or surface
$\infty, 0$ = freestream condition
η = differentiation with respect to η

Superscripts

$(\ )^*$ = dimensionless quantities

I. Introduction

THE flow of partially ionized gases over solid bodies and through channels has been a subject of considerable interest in recent years owing to its wide applications, e.g., in high-temperature material processing, magnetoplasma devices, and high-speed flight vehicles. The flow problems associated with ionized gases can be classified broadly into two groups. The first one deals with laminar boundary-layer flows of an ionized gas over bodies and includes the side-wall and end-wall boundary layers induced by a shock wave. The study of flows (subsonic and supersonic) over blunt bodies—as in Langmuir type probes, anodes, or such bodies where stagnation-point analysis is considered—forms the second group. In the study of the above, concepts of viscous and thermal layer are employed where either a single- or a multifluid approach is used. The complexities of the problem herein depend on the number of energy transport mechanisms of species in the presence of the application of external electric and/or magnetic fields, if any. In earlier works, plasma nonequilibrium transport properties based on Fay's mixture rule[1] or mean free path methods were employed to solve a system of single- or

Received April 9, 1983; revision received Aug. 18, 1983. Copyright © American Institute of Aeronautics and Astronautics, Inc., 1983. All rights reserved.

*Professor, Department of Aeronautical Engineering. Associate Fellow AIAA.

†Research Scholar, Department of Aeronautical Engineering; currently, Assistant Professor, Department of Mechanical Engineering, College of Engineering, Guindy, Anna University, Madras.

multifluid equations. However, the existence of thermal nonequilibrium of species characterized by separate kinetic temperatures in a collision-dominated plasma demands special attention to transport property calculations. It is discussed briefly in Sec. III.

The present study concerns two-temperature plasma heat transfer to the stagnation point of an axisymmetric blunt body in a subsonic, high-enthalpy flow with joule heating. A typical example of this flow situation is the anode region which is initially marked by a diversion of the plasma stream in a stagnation-like flow. In the present analysis a multifluid model is employed and is solved numerically for the case of argon using the most recent updated transport properties. To the authors' knowledge, the present study of a stagnation-point boundary-layer problem with joule heating employing two-temperature transport properties is the first to appear.

A brief literature survey on partially ionized gas boundary-layer flow is made. In Sec. III, a brief discussion of two-temperature thermodynamic and transport properties is presented. In Sec. IV, formulation of the problem is presented, and the assumptions are stated; the numerical scheme is discussed in Sec. V. Finally, the results obtained for various problem parameters are discussed in Sec. VI.

II. Review of Previous Work

The present review pertains to boundary-layer problems in ionized gases only and is not intended to be an exhaustive one. Fay and Kemp[2,3] studied the stagnation-point heat transfer in a partially ionized gas for frozen and equilibrium conditions. Also studied was the heat transfer to a shock tube end wall for an ionizing monatomic gas. Okuno and Park[4] presented a two-temperature theory and experimental results for the heat transfer to the stagnation point of a hemisphere in a supersonic high-enthalpy dissociating and ionizing nitrogen plasma flow. Sherman and Reshotko[5] obtained the electron temperature profiles for flow in chemical equilibrium over a flat plate on the basis of a similar solution. Tseng and Talbot[6] performed a combined numerical and experimental investigation on flat-plate boundary-layer flow of a partially ionized gas using constant-temperature transport properties. Bose[7] investigated theoretically the heat transfer from a preionized gaseous plasma flowing over an anode at an elevated electron temperature in the presence of an electric field. The present formulation for a stagnation-point boundary layer is based on the multifluid approach presented in the above work. Talbot[8] carried out a theoretical study of a stagnation-point boundary layer of a Langmuir probe. He used the assumption of thermal equilibrium in the boundary layer. Chung[9] analyzed the stagnation-point boundary layer, separating it into ambipolar and sheath regions under equilibrium conditions. Knight[10] showed the effect of reactions, collisions, and electron reflection on the electron heat transfer and temperature.

III. Two-Temperature Thermodynamic and Transport Coefficients

In this section, we give the thermodynamic properties of a two-temperature ionized gas and explain the physical basis for the diffusion and reactive heat conductivity expressions for the transport properties used in the numerical calculations.

Thermodynamic Properties

In the present work on a collision-dominated, three-component plasma, the dominant modes of energy storage are the species thermal energy and the ionization energy. The thermodynamic and caloric equations of state are

$$p = n_e k_B T_e + k_B T_h \sum_{j \in H} n_j \tag{1}$$

$$h_j = \frac{5}{2}\frac{k_B T_j}{m_j}$$

where $j \in H$ means that j belongs to a set of heavy particles. The enthalpy of the mixture becomes

$$h_j = \tfrac{5}{2} R T_h / m_h + h_{j,\mathrm{exc}} + h_{j,0}, \qquad j \in H \tag{2}$$

where $h_{j,\mathrm{exc}}$ and $h_{j,0}$ are the excitation energy and the heat of formation at 0 K, respectively.

The following approximations and definitions are used:

$$(m_e/m_i) \ll 1, \qquad m_i \simeq m_n, \qquad n_e \simeq n_i$$

$$\alpha = n_e/(n_e + n_n), \qquad m_j = RM_j/k_B$$

$$\rho = \Sigma n_j M_j = (k_B n/R)\Sigma x_j m_j \tag{3}$$

where R and α are universal gas constant and degree of ionization, respectively.

Numerical computation of transport properties requires an accurate evaluation of plasma composition. We have used the Monti-Napolitano-Veis[11,12] equilibrium composition model to calculate composition and use them in species transport properties evaluation.[13-15] Out of the analysis for a two-temperature plasma, the following relations are obtained for ambipolar diffusion coefficient and species reactive or diffusion heat conductivity coefficients:

$$D_{\mathrm{amb}} = i[1 + \theta x_{i+1}/x_i] D_{i+1} \tag{4}$$

$$k_{re} = \frac{(nD_{\mathrm{amb}})}{N_A}[H_e + H_{i+1} - H_i]\frac{\partial x_e}{\partial T_e} \tag{5}$$

$$k_{rh} = \frac{(nD_{\mathrm{amb}})}{N_A}[H_e + H_{i+1} - H_i]\frac{\partial x_e}{\partial T_h} \tag{6}$$

The subscripts $i = 1$ and $i = 2$ correspond to neutrals and singly charged ions, respectively.

The total heat flux due to conduction and diffusion, in the absence of radiation, can now be written in terms of species temperature gradients as

$$\begin{aligned} q &= -k_{ch}\nabla T_h - k_{ce}\nabla T_e + \sum_{j=e,H} \rho_j V_j' h_j \\ &= -(k_{ch} + k_{rh})\nabla T_h - (k_{ce} + k_{re})\nabla T_e \\ &= -k_h \nabla T_h - k_e \nabla T_e \end{aligned} \tag{7}$$

Transport Properties

Based on the Chapman-Enskog-Burnett method, Devoto[16] presented simplified expressions and numerical results for transport properties of equilibrium partially ionized argon. Kannappan and Bose[13,14] reported the transport properties of argon and helium two-temperature plasmas over a wide range of temperatures and pressures. However, their analysis was restricted to an electron-to-heavies temperature ratio of 3, and also to pure heat conduction coefficients only. In the present work, properties were obtained according to Refs. 13 and 14, except with the modifications shown in Eqs. (4-6) for θ values up to 16; such high values occur at plasma boundaries where the electron temperature is high.

IV. Formulation of the Problem

Under the steady axisymmetric flow conditions shown in Fig. 1 the freestream gas is in thermal equilibrium and in a partially ionized state. For a blunt body placed in the above flow conditions, a laminar, two-temperature, stagnation-point boundary layer is formed in which an interaction between thermal and viscous layers occurs in the presence of joule heating.

In accordance with the aforementioned flow model, the following assumptions are introduced in the analysis:

1) The gas is composed of argon atoms, ions, and electrons in chemical equilibrium, the electrons being the principal current carrier.

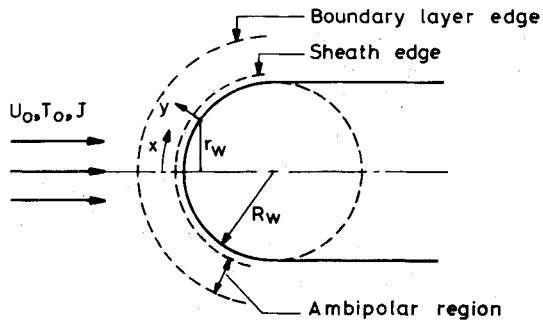

Fig. 1 Axisymmetric laminar stagnation-point boundary-layer flow model. (For clarity the ambipolar region is shown magnified.)

2) There is ambipolar diffusion in the boundary layer so that $n_e = n_i$ (quasineutrality).

3) $T_a = T_i = T_h$. Local thermodynamic equilibrium (LTE) prevails in the freestream.

4) The freestream static temperature near the stagnation point is constant along the x direction and is equal to that at the stagnation point.

5) Sheath thickness is negligible compared to boundary-layer thickness, which in turn is very small compared to the radius of curvature of the body.

6) A one-dimensional approach for the electric current flow is possible near the surface since the electric current density normal to the wall is constant.

7) There is no blowing or suction on the wall.

The boundary-layer equations for an axisymmetric laminar two-temperature plasma flow in the presence of an electric field are as follows:

Continuity

$$\frac{\partial}{\partial x}(\rho u r_w) + \frac{\partial}{\partial y}(\rho v r_w) = 0 \tag{8}$$

Momentum

$$\rho u \frac{\partial u}{\partial x} + \rho v \frac{\partial u}{\partial y} = -\rho_0 U_0 \frac{\mathrm{d}U_0}{\mathrm{d}x} + \frac{\partial}{\partial y}\left(\mu \frac{\partial u}{\partial y}\right) \tag{9}$$

Global energy

$$\rho u \frac{\partial h}{\partial x} + \rho v \frac{\partial h}{\partial y} = \frac{\partial}{\partial y}\left(k_e \frac{\partial T_e}{\partial y}\right) + \frac{\partial}{\partial y}\left(k_h \frac{\partial T_h}{\partial y}\right) + \frac{J^2}{\sigma} \tag{10}$$

Electron energy

$$\frac{\partial}{\partial y}\left(k_e \frac{\partial T_e}{\partial y}\right) = 3\frac{m_e}{m_h} k_B (T_e - T_h)\Gamma_{eh} + \frac{5}{2}\frac{k_B}{e} J \frac{\partial T_e}{\partial y} - \frac{J^2}{\sigma}(1 - \alpha_2) \tag{11}$$

Global energy – electron energy

$$\rho u \frac{\partial h}{\partial x} + \rho v \frac{\partial h}{\partial y} = \frac{\partial}{\partial y}\left(k_h \frac{\partial T_h}{\partial y}\right) + \frac{5}{2}\frac{k_B}{e} J \frac{\partial T_e}{\partial y} + 3\frac{m_e}{m_h} k_B (T_e - T_h)\Gamma_{eh} + \frac{J^2}{\sigma}\alpha_2 \tag{12}$$

Since $\rho_e \ll \rho_h$, the terms $\rho_e u_e \partial h_e/\partial x$ and $\rho_e v_e \partial h_e/\partial y$ are neglected *in comparison* with the corresponding terms in the heavies energy equation. Further, current relations with sign conventions are given in the Appendix.

Boundary conditions

$$y = 0, \qquad u = v = 0, \qquad T_h = T_w$$

$$-k_e \frac{\partial T_e}{\partial y}\bigg|_b = c_{pi,\mathrm{transl}} \rho_i V_i' \left[0.4 \frac{e\varphi}{k_B T_e} - 0.2\right] T_{e(y=b)}$$

$$y \to \infty, \qquad u = U_0, \qquad T_e = T_0 + J^2 m_h / (3 m_e k_B \sigma_0 \Gamma_{eH_0}) \tag{13}$$

If the wall surface considered is an anode, there would be a sizable contribution to the heat flux due to $5k_B T_e J/2e$, but this contribution does not go into the calculation at this stage. The boundary condition for the electron energy equation is obtained from continuity of the electron energy flux at the sheath edge between continuum and molecular descriptions.

In order to obtain similar solutions near the stagnation point, the following transformation coordinates are introduced:

$$\eta = \frac{(\rho U)_0 r_w}{\sqrt{2s}} \int_0^y \frac{\rho}{\rho_0}\,\mathrm{d}y$$

$$s = \int_0^x (\rho\mu U)_0 r_w^2\,\mathrm{d}x \tag{14}$$

In addition, the following dimensionless quantities and definitions are introduced:

$$f_\eta = u/U_0,\ T_e^* = (T_e - T_0)/(T_0 - T_w)$$

$$T_h^* = (T_h - T_0)/(T_0 - T_w)$$

$$h^* = (h - h_w)/(h_0 - h_w)$$

$$\sigma^* = \sigma/\sigma_0,\ \Gamma_{eH}^* = \Gamma_{eH}/\Gamma_{eH_0}$$

$$\rho^* = \rho/\rho_0,\ C = \mu\rho/(\mu\rho)_0,\ \langle c_p\rangle = (h_0 - h_w)/(T_0 - T_w)$$

$$Pr_e = \mu\langle c_p\rangle/k_e,\ Pr_h = \mu\langle c_p\rangle/k_h,\ Re = (U\rho/\mu)_0 R_w \tag{15}$$

where subscripts 0 and w refer to freestream and wall conditions, respectively.

The following constants are obtained in the process of normalizing and coordinate transformation of the system of equations:

$$k_1 = \frac{5}{2\sqrt{3}}\frac{k_B}{e}\frac{R_w J}{\mu_0\langle c_p\rangle};\qquad k_2 = \frac{e}{\sqrt{3}}\frac{R_w J}{\mu_0\langle c_p\rangle}\left(\frac{nD_{\mathrm{amb}}}{\sigma}\right)_0$$

$$k_3 = \frac{m_e}{m_h}\frac{k_B R_w^2 \Gamma_{eH_0}}{\mu_0\langle c_p\rangle};\qquad k_4 = \frac{1}{3}\frac{R_w^2 J^2}{(T_0 - T_w)(\sigma\mu)_0\langle c_p\rangle}$$

$$k_5 = \frac{1}{2}\ln\left(\theta_b \frac{m_h}{m_e}\right);\qquad k_6 = \frac{5}{2}\frac{k_B}{e}\left(\frac{nD_{\mathrm{amb}}}{k_e}\right)_0 (0.4k_5 - 0.2) \tag{16}$$

The transformed dimensionless system of equations and the boundary conditions are as follows:

$$ff_{\eta\eta} + (Cf_{\eta\eta})_\eta + \tfrac{1}{2}(\rho_0/\rho - f_\eta^2) = 0 \tag{17}$$

$$fh_\eta^* + \left(\frac{C}{Pr_h} T_{h_\eta}^*\right)_\eta + \frac{k_1}{\sqrt{Re}} T_{e_\eta}^* - \frac{k_2}{\sqrt{Re}}\left(\frac{nD_{\mathrm{amb}}^*}{\sigma}\right) \times \left[\frac{\partial x_e}{\partial T_e}\frac{\mathrm{d}T_e^*}{\mathrm{d}\eta} + \frac{\partial x_e}{\partial T_h}\frac{\mathrm{d}T_h^*}{\mathrm{d}\eta}\right] + k_3 \frac{\rho_0}{\rho}\frac{1}{Re}(T_e^* - T_h^*)\Gamma_{eH}^* = 0 \tag{18}$$

$$\left(\frac{C}{Pr_e}T^*_{e_\eta}\right)_\eta - \frac{k_1}{\sqrt{Re}}T^*_{e_\eta} + \frac{k_2}{\sqrt{Re}}\left(\frac{nD_{\text{amb}}}{\sigma}\right)^*\left[\frac{\partial x_e}{\partial T_e}\frac{\mathrm{d}T^*_e}{\mathrm{d}\eta} + \frac{\partial x_e}{\partial T_h}\frac{\mathrm{d}T^*_h}{\mathrm{d}\eta}\right] + \frac{k_4\rho_0}{Re\rho}\frac{1}{\sigma^*} - \frac{k_3\rho_0}{Re\rho}(T^*_e - T^*_h)\Gamma^*_{eH} = 0 \quad (19)$$

$$\eta = 0: f = f_\eta = 0; \qquad T^*_h = h^*$$

$$k_e T^*_{e_\eta} = k_6(nD_{\text{amb}})^*_w(T^*_{e_w} + \Delta)x_{e_\eta} \quad (20)$$

$$\eta \to \infty: f_\eta = 1, \qquad T^*_h = h^* = 1$$

$$T^*_e = 1 + \left\{J^2 \Big/ \sigma_0\left[3\frac{m_e}{m_h}k_B(T_0 - T_w)\Gamma_{eH_0}\right]\right\} \quad (21)$$

In Eq. (17), the factor $\frac{1}{2}$ is the value of the pressure gradient parameter at the stagnation point for an axisymmetric blunt-body problem (strictly for the stagnation point of a sphere of radius R_w).

According to the usual definitions employed in boundary-layer theory, the following expressions are obtained:

$$y = \frac{R_w}{\sqrt{3Re}}\int_0^\eta \rho^{*-1}\,\mathrm{d}\eta \quad (22)$$

Displacement thickness

$$\delta_1 = \frac{R_w}{\sqrt{3Re}}\int_0^\eta \left[(1 - \rho^* f_\eta)/\rho^*\right]\mathrm{d}\eta \quad (23)$$

Momentum thickness

$$\delta_2 = \frac{R_w}{\sqrt{3Re}}\int_0^\eta f_\eta(1 - f_\eta)\,\mathrm{d}\eta \quad (24)$$

From the condition of continuity of current and electrical conductivity and velocity variations within the boundary layer, the potential drop is given by

$$\delta\varphi = \int_0^\infty (E - E_0)\,\mathrm{d}y = \frac{J}{\sigma_0}\frac{R_w}{\sqrt{3Re}}\int_0^\infty [(1/\sigma^* - 1)/\rho^*]\,\mathrm{d}\eta \quad (25)$$

Among all the energy transport mechanisms near the wall, such as heat transport due to heavies, electrons, diffusion of electrons, and recombination energy due to diffusion of ions, the heavy particle heat transfer is found to be dominant. In view of the insensitivity demonstrated by the sheath boundary condition to $T^*_e(0)$, use of the condition $\mathrm{d}T^*_e/\mathrm{d}\eta = 0$ at $\eta = 0$ in obtaining the electron temperature profile appears justified. Furthermore, Nishida[17,18] has also shown that the electron temperature gradient at the wall is negligibly small, so that electron contribution to wall heat transfer becomes negligible. It is given by

$$q_w = -\frac{\sqrt{3Re}}{R_w}\frac{(\rho k_h)_w}{\rho_0}T^*_{h\eta}(0) \quad (26)$$

$$St = -\frac{\sqrt{3}\,C_w}{Pr_h\sqrt{Re}}T^*_{h\eta} \quad (27)$$

V. Numerical Scheme

The governing equations of the problem considered are a set of coupled, nonlinear second-order ordinary differential equations. A finite difference quasilinearized representation of electron and heavies energy equations is written for each grid point, to be solved simultaneously. The momentum equation is integrated by the Runge-Kutta method. In this, the initial condition f_η ($\eta = 0$) is adjusted for each iteration for given T^*_e and T^*_h profiles such that the other boundary condition is satisfied. This "shooting technique" of solving the momentum equation is well established in solving boundary-layer equations. Further updating of T^*_e and T^*_h profiles is done by solving Eqs. (18) and (19) in finite difference form.

The procedure is repeated until convergence to the required accuracy is achieved. After the profiles are computed for a given set of freestream conditions, a number of integral quantities such as δ_1, δ_2, $\delta\varphi$, and Stanton number are evaluated. Each computer run took roughly 7 min for nine iterations and relative error between successive iterates was less than 10^{-3}. The computations described above were carried out for the following range of conditions:

$p = 0.1$ and 1 bar, $\quad T_w = 1{,}000$ K

$R_w = 0.01$ m, $\quad U_0 = 30$ m/s

$J = 10^4$-10^6 A/m^2, $\quad T_0 = 12{,}000$ K and 16,000 K

VI. Calculated Results and Discussion

The parameters of the present problem that can be specified independently to study the thermal nonequilibrium characteristics are freestream temperature T_0, radius R_w, current density J, and pressure p. A solution procedure for a given set of parameters consists of obtaining f, f_η, $f_{\eta\eta}$, T^*_e, T^*_h, and thermodynamic and transport properties at every grid point and further calculating the quantities δ_1, δ_2, $\delta\varphi$, and St. Since the total volume of numerical results is large, only a few representative results are plotted here and are discussed.

Figures 2a and 2b present boundary-layer profiles of nondimensional electron and heavies temperatures and velocity. It may be seen that the electron temperature at $\eta = 0$ is significantly above the heavy particles temperature, and it is of the order of 80% of the nondimensional freestream temperature. The effect of parameter J on the species' temperatures and velocity profiles is also shown in Figs. 2a and 2b for two different freestream temperatures, from which it is seen that the effect of current on species temperature variation is greater at $T_0 = 12{,}000$ K over that at $T_0 = 16{,}000$ K. The major effect of increased joule heating is in raising the electron temperature across the boundary layer. It was found, however, that at low current densities T^*_e and T^*_h profiles become independent of J. (This result is very important for Langmuir probe diagnostics.) We also note that this high value of T^*_e at the wall at low current densities comes out of the numerical solution of the electron energy equation, since the heat flux by the conducting electrons does not get dissipated by the collisional energy exchange term in the energy equation. Further, the location at which T^*_e departs from T^*_h is nearer to the wall with increasing current at a given T_0. Also, the difference between T_e and T_h, which is a measure of the severity of thermal nonequilibrium, is observed to be greater at higher currents. This ensures the gas to be a satisfactory conductor near the surface.

At pressure $p < 1$ bar, it is found that the point of departure moves away from the wall and there is a higher electron surface temperature, indicating that the electrons and heavies thermally relax over an appreciable portion of the boundary-layer region. Our calculations show the temperature excess ($T^*_e > 1$) near the edge of the boundary layer for higher currents at $p < 1$ bar. A plausible explanation for this is that joulean heat addition is being blocked from transfer to the wall by the low electron thermal conductivity.

Figure 3 shows the variations of Pr_e, Pr_h, C, and Γ^*_{eH} across the boundary layer. The variation of the viscosity density product ratio C (also referred to as a Chapman-Rubesin factor) is the one which influences the velocity profile in the boundary layer and can be of importance for stability of flow in a nonstagnation region. At $T_0 = 16{,}000$ K the value

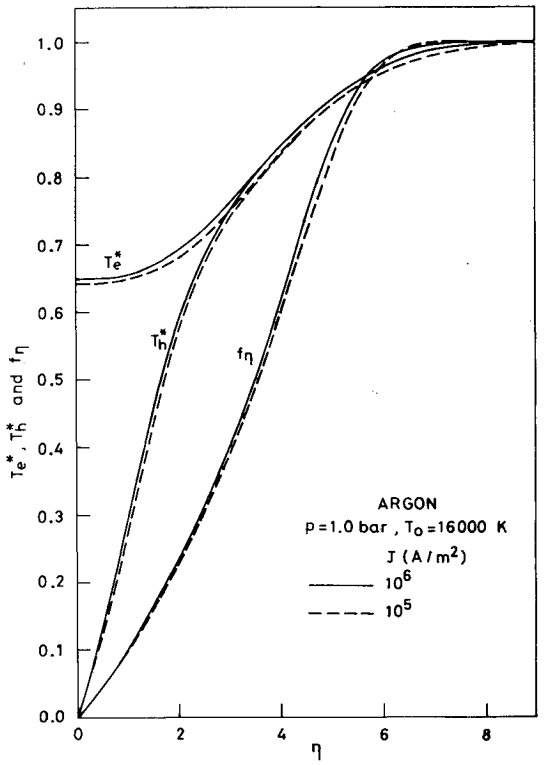

Fig. 2a Normalized profiles of the velocity f_η, the heavies temperature T_h^*, and the electron temperature T_e^* for $p = 1$ bar and $T_0 = 16{,}000$ K.

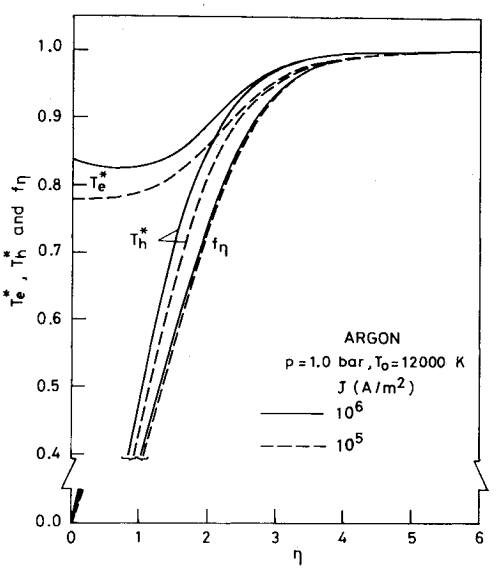

Fig. 2b Normalized profiles of the velocity f_η, the heavies temperature T_h^*, and the electron temperature T_e^* for $p = 1.0$ bar and $T_0 = 12{,}000$ K.

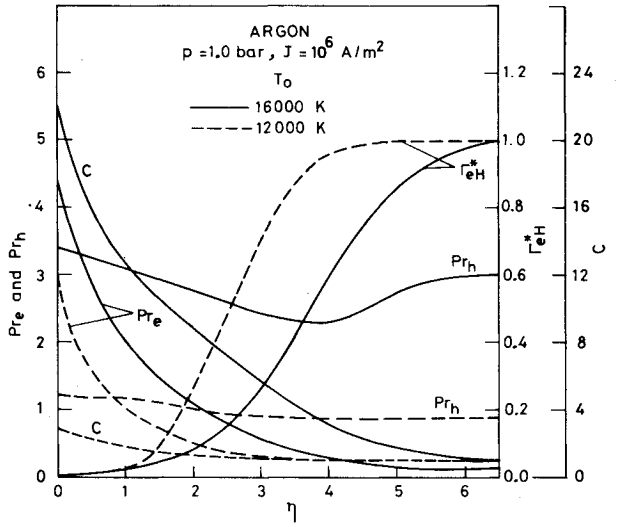

Fig. 3 C, Pr_e, Pr_h, and Γ_{eH}^* vs η for $T_0 = 12{,}000$ and 16,000 K, $p = 1.0$ bar, $J = 10^6$ A/m².

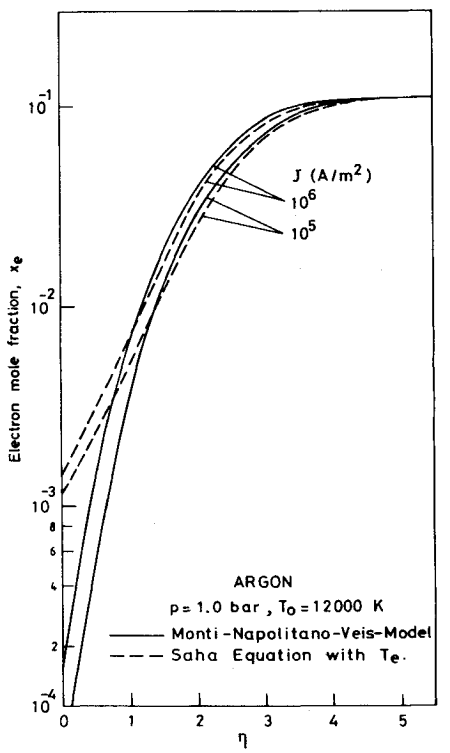

Fig. 4 Electron mole fraction profiles for $p = 1.0$ bar, $T_0 = 12{,}000$ K, $J = 10^5$ and 10^6 A/m².

of C near the surface is 20 times that at freestream conditions, whereas the corresponding value is 3 for $T_0 = 12{,}000$ K. This wide variation in C due to species temperature variation brings about appreciable changes in the velocity field, as shown in Fig. 2. Although the electron subgas Prandtl number variation is similar, it has higher values near the wall for higher freestream temperature. The heavies Prandtl number remains constant across the boundary layer at $T_0 = 12{,}000$ K, whereas its variation becomes significant at $T_0 = 16{,}000$ K. In the calculation of Pr, $\langle c_p \rangle$ is the average value calculated from mixture enthalpy, the viscosity corresponds to heavies only (the contribution of electrons to the mixture viscosity is neglected since $\mu_j \propto \sqrt{m_j}$), and the calculation of k_e and k_h includes the reactive part of heat conductivity coefficients shown in Eqs. (5) and (6).

Although the variation of electron-heavies volumetric collision frequency is almost similar for the parameters shown in Fig. 4, it is seen that the relative or dimensionless elastic collision energy exchange is more for a given current at a given location at lower freestream temperature (for $J = 10^6$ A/m² at $\eta = 3$, $\Gamma_{eH}^* = 0.26$ and 0.36 at $T_0 = 16{,}000$ and 12,000 K, respectively).

A significant feature of Fig. 4 is the fact that the electron mole fraction computed from the Monti-Napolitano-Veis model near the surface is much different from that evaluated with the help of a model in which T_e replaces T in the Saha equation. Also shown in Fig. 4 is the effect of increased current to increase the electron mole fraction. The diffusion flux in the ambipolar region is calculated from Eq. (A3), and

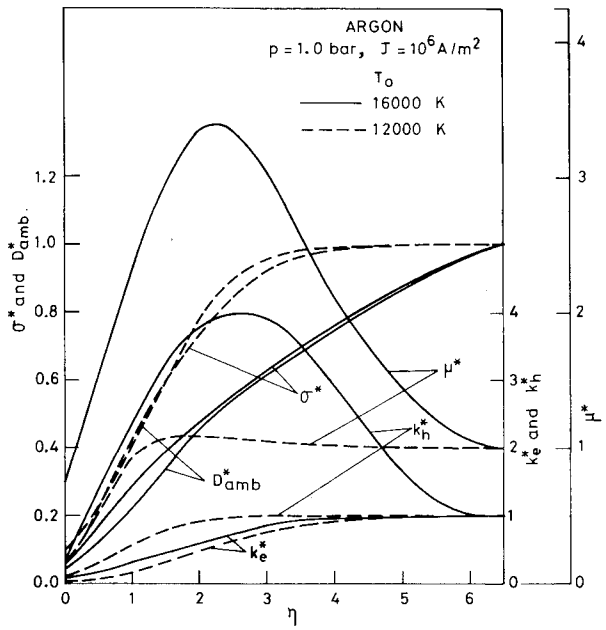

Fig. 5 Typical variation of normalized transport coefficients in the boundary layer for $T_0 = 12{,}000$ and 16,000 K, $p = 1.0$ bar, $J = 10^6$ A/m^2.

Table 1 Thermodynamic and transport properties of two-temperature argon plasma in freestream at $p = 1$ bar

	$T_0 = 12{,}000$ K	$T_0 = 16{,}000$ K
D_{amb}, m^2/s	4.462×10^{-3}	6.797×10^{-3}
k_e, W/mK	1.113	2.093
k_h, W/mK	3.028×10^{-1}	5.413×10^{-2}
σ, mho/m	4.786×10^{3}	8.221×10^{3}
μ, kg/m/s	2.688×10^{-4}	8.058×10^{-5}
Γ_{eH}, m^{-3}s^{-1}	3.016×10^{34}	1.686×10^{35}
At $J = 10^6$ A/m^2		
δ_1	1.591×10^{-4}	1.974×10^{-4}
δ_2	4.531×10^{-4}	6.567×10^{-4}
$\delta\varphi$	3.03×10^{-1}	1.571×10^{-1}
St	2.397×10^{-1}	2.909×10^{-1}

represents an upper limit for a chemically relaxing flow situation.

Figure 5 shows a typical variation of nondimensional transport properties of two-temperature argon plasma across the stagnation-point boundary layer. These transport properties are functions of T_e, T_h, p, n_e, and n_n, and are given as input values to a separate subroutine program to supply the local values of the transport coefficients in solving the species' energy equations. Since these properties are nondimensionalized with respect to those in the freestream, the latter can be obtained from Table 1, which provides the transport properties for $T_0 = 16{,}000$ and 12,000 K at $p = 1$ bar. Also shown in Table 1 are the values of δ_1, δ_2, $\delta\varphi$, and St for various current densities.

Near the surface, the heat conductivity coefficient for heavy particles has a finite value, whereas for electrons, although finite, it is negligible compared to that of heavies. This is because the electron mole fraction becomes smaller as one approaches the wall surface.

For the continuity of current density across the boundary layer, joule heating, which varies inversely with σ, is high near the surface. This leads to a higher electron surface temperature, but the electron heat conductivity coefficient is so small that the surface may be taken as insulated for the electron subgas. In summary, a method to calculate a stagnation-point, two-temperature boundary layer has been given and results of calculation for a two-temperature argon plasma are presented, highlighting some of the important results.

Appendix—Current Densities, Mobility, and Diffusion Coefficients

The following sign convention and current relations are employed in the boundary-layer equations. The externally applied electric field is

$$\boldsymbol{E} = -\nabla\varphi \tag{A1}$$

Electron and ion field and diffusion currents are

$$\boldsymbol{J} \simeq \boldsymbol{J}_{fe} = \sigma\boldsymbol{E} = en_e b_e \boldsymbol{E}$$

$$\boldsymbol{J}_{fi} = en_e b_i \boldsymbol{E}$$

$$\boldsymbol{J}_{d_i} = -\boldsymbol{J}_{d_e} = -enD_{\text{amb}}\nabla x_e \tag{A2}$$

Flux of diffusing electron-ion pairs in the ambipolar region shown in Fig. 1 is

$$\boldsymbol{F}_w = m_i n_i \boldsymbol{V}' = -m_i n_i D_{\text{amb}} \frac{1}{x_e}\frac{\mathrm{d}x_e}{\mathrm{d}y} \tag{A3}$$

The following are the expressions for D_j, b_j, and D_{amb} derived for a two-temperature plasma:

$$D_i = D_{\text{amb}}/(1+\theta);\ D_e = k_B T_e \sigma/(e^2 n_e)$$

$$b_i = eD_{\text{amb}}/[k_B T_h(1+\theta)];\ b_e = \sigma/(en_e)$$

$$D_{\text{amb}} = D_i(1+\theta) \tag{A4}$$

The following current ratios are defined:

$$\alpha_1 = \boldsymbol{J}_{fi}/\boldsymbol{J} = e^2 n_e D_{\text{amb}}/[k_B T_h(1+\theta)]$$

$$\alpha_2 = \boldsymbol{J}_d/\boldsymbol{J} \tag{A5}$$

The ion and electron current relations with the above definitions are written as

$$\boldsymbol{J}_i = \boldsymbol{J}(\alpha_1 + \alpha_2) \simeq \alpha_2 \boldsymbol{J}$$

$$\boldsymbol{J}_e = \boldsymbol{J}(1 - \alpha_2) \tag{A6}$$

Acknowledgments

This work forms a part of the Ph.D. work of the second author, who wishes to acknowledge the support of the Ministry of Education, Government of India, and also the authorities of Anna University, Madras, for deputation. Also, the help of the Computer Centre, IIT Madras, for providing ample time for the numerical computation is gratefully acknowledged.

References

[1]Fay, J.A., "Hypersonic Heat Transfer in the Air Laminar Boundary Layer," *The High Temperature Aspects of Hypersonic Flow*, edited by W.C. Nelson, Macmillan Book Co., New York, 1964, Chap. 30.

[2]Fay, J.A. and Kemp, N.H., "Theory of Stagnation-Point Heat Transfer in a Partially Ionized Diatomic Gas," *AIAA Journal*, Vol. 1, 1963, pp. 2741-2751.

[3]Fay, J.A. and Kemp, H., "Theory of Heat Transfer to a Shock-tube End-wall from an Ionized Monatomic Gas," *Journal of Fluid Mechanics*, Vol. 21, Pt 4, 1965, pp. 659-672.

[4]Okuno, F.A. and Park, C., "Stagnation-Point Heat Transfer Rate in Nitrogen Plasma Flows: Theory and Experiment," *ASME Journal of Heat Transfer*, Vol. 92, Aug. 1970, pp. 372-384.

[5]Sherman, A. and Reshotko, E., "Nonequilibrium Boundary Layer along an Insulator Wall," *AIAA Journal*, Vol. 7, March 1969, pp. 610-615.

[6]Tseng, R.C. and Talbot, L., "Flat Plate Boundary-Layer Studies in a Partially Ionized Gas," *AIAA Journal*, Vol. 7, July 1971, pp. 1365-1372.

[7]Bose, T.K., "Anode Heat Transfer for a Flowing Argon Plasma at Elevated Electron Temperature," *International Journal of Heat and Mass Transfer*, Vol. 15, Nov. 1972, pp. 1745-1763.

[8]Talbot, L., "Theory of the Stagnation-Point Langmuir Probe," *Physics of Fluids*, Vol. 3, March 1960, pp. 289-298.

[9]Chung, P.M., "Electrical Characteristics of Coutte and Stagnation Boundary Layer Flows of Weakly Ionized Gas," *Physics of Fluids*, Vol. 14, Jan. 1964, pp. 110-120.

[10]Knight, D.D., "Electron Thermochemical Nonequilibrium Effects in Re-entry Boundary Layers," *AIAA Journal*, Vol. 2, Feb. 1971, pp. 193-199.

[11]Monti, R. and Napolitano, L.G., "Generalized Saha Equation for Nonequilibrium Two-Temperature Plasmas," *XV International Astronomy Congress (1964)*. AGARD, Cannes, France, March 1964, pp. 517-537 (AGARDOGRAPH 81).

[12]Veis, S., "The Saha Equation and Lowering of Ionization Energy for a Two-Temperature Plasma," *Czechoslovak Conference on Electronics and Vacuum Physics, Proceedings 105*, 1968.

[13]Kannappan, D. and Bose, T.K., "Transport Properties of a Two-Temperature Argon Gas," *Physics of Fluids*, Vol. 20, Oct. 1977, pp. 1668-1673.

[14]Kannappan, D. and Bose, T.K., "Transport Properties of a Two-Temperature Helium Plasma," *Physics of Fluids*, Vol. 23, July 1980, pp. 1473-1474.

[15]Igra, O. and Barcessat, M., "Supersonic Nonequilibrium Corner Expansion Flow of Ionized Argon," *Physics of Fluids*, Vol. 20, Sept. 1977, pp. 1449-1457.

[16]Devoto, R.S., "Transport Coefficients of Partially Ionized Argon," *Physics of Fluids*, Vol. 10, Feb. 1967, pp. 354-364.

[17]Nishida, M. and Matsuoka, K., "Structure of Nonequilibrium Boundary Layer along a Flat Plate in a Partially Ionized Gas," *AIAA Journal*, Vol. 9, Nov. 1971, pp. 3117-3118.

[18]Nishida, M. and Sugimoto, S., "Electron Temperature Measurements along a Stagnation Point Stream Line," *Physics of Fluids*, Vol. 16, Feb. 1973, pp. 202-204.

From the AIAA Progress in Astronautics and Aeronautics Series . . .

GASDYNAMICS OF DETONATIONS AND EXPLOSIONS—v. 75
and
COMBUSTION IN REACTIVE SYSTEMS—v. 76

Edited by J. Ray Bowen, University of Wisconsin,
N. Manson, Université de Poitiers,
A. K. Oppenheim, University of California,
and R. I. Soloukhin, BSSR Academy of Sciences

The papers in Volumes 75 and 76 of this Series comprise, on a selective basis, the revised and edited manuscripts of the presentations made at the 7th International Colloquium on Gasdynamics of Explosions and Reactive Systems, held in Göttingen, Germany, in August 1979. In the general field of combustion and flames, the phenomena of explosions and detonations involve some of the most complex processes ever to challenge the combustion scientist or gasdynamicist, simply for the reason that *both* gasdynamics and chemical reaction kinetics occur in an interactive manner in a very short time.

It has been only in the past two decades or so that research in the field of explosion phenomena has made substantial progress, largely due to advances in fast-response solid-state instrumentation for diagnostic experimentation and high-capacity electronic digital computers for carrying out complex theoretical studies. As the pace of such explosion research quickened, it became evident to research scientists on a broad international scale that it would be desirable to hold a regular series of international conferences devoted specifically to this aspect of combustion science (which might equally be called a special aspect of fluid-mechanical science). As the series continued to develop over the years, the topics included such special phenomena as liquid- and solid-phase explosions, initiation and ignition, nonequilibrium processes, turbulence effects, propagation of explosive waves, the detailed gasdynamic structure of detonation waves, and so on. These topics, as well as others, are included in the present two volumes. Volume 75, *Gasdynamics of Detonations and Explosions,* covers wall and confinement effects, liquid- and solid-phase phenomena, and cellular structure of detonations; Volume 76, *Combustion in Reactive Systems*, covers nonequilibrium processes, ignition, turbulence, propagation phenomena, and detailed kinetic modeling. The two volumes are recommended to the attention not only of combustion scientists in general but also to those concerned with the evolving interdisciplinary field of reactive gasdynamics.

Volume 75—468 pp., 6×9, illus., $30.00 Mem., $45.00 List
Volume 76—688 pp., 6×9, illus., $30.00 Mem., $45.00 List
Set—$60.00 Mem., $75.00 List

TO ORDER WRITE: Publications Order Dept., AIAA, 1633 Broadway, New York, N.Y. 10019